Relation between oxidation microstructure and the maximum energy product loss of a Sm_2Co_{17} magnet oxidized at 500 °C*

Liu Li-Li(刘丽丽) and Jiang Cheng-Bao(蒋成保)†

Key Laboratory of Aerospace Materials and Performance (Ministry of Education), School of Materials Science and Engineering, Beihang University, Beijing 100191, *China*

(Received 22 June 2011; revised manuscript received 22 July 2011)

The oxidation microstructure and maximum energy product $(BH)_{max}$ loss of a $Sm(Co_{0.76}, Fe_{0.1}, Cu_{0.1}, Zr_{0.04})_7$ magnet oxidized at 500 °C were systematically investigated. Three different oxidation regions were formed in the oxidized magnet: a continuous external oxide scale, an internal reaction layer, and a diffusion zone. Both room-temperature and high-temperature $(BH)_{max}$ losses exhibited the same parabolic increase with oxidation time. An oxygen diffusion model was proposed to simulate the dependence of $(BH)_{max}$ loss on oxidation time. It is found that the external oxide scale has little effect on the $(BH)_{max}$ loss, and both the internal reaction layer and diffusion zone result in the $(BH)_{max}$ loss. Moreover, the diffusion zone leads to more $(BH)_{max}$ loss than the internal reaction layer. The values of the oxidation rate constant k for internal reaction layer and oxygen diffusion coefficient D for diffusion zone were obtained, which are about 1.91×10^{-10} cm^2/s and 6.54×10^{-11} cm^2/s, respectively.

Keywords: Sm_2Co_{17} magnet, maximum energy product loss, internal reaction layer, diffusion zone

PACS: 75.50.Ww, 75.60.Ej, 81.65.Mq, 66.30.–h **DOI:** 10.1088/1674-1056/20/12/127502

1. Introduction

With an increasing demand for a high-temperature permanent magnets operating at 500 °C, a renewed interest in Sm_2Co_{17}-type magnets has developed.[1−5] Due to a nanoscale cellular–lamellar structure consisting of a rhombohedral $Sm_2(Co, Fe)_{17}$ cell phase, a hexagonal $Sm(Co, Cu)_5$ cell boundary phase and a lamellar Z-phase, the Sm_2Co_{17}-type magnet has a high Curie temperature and low temperature dependence of the remanence. There were extensive studies on optimizing the alloy composition, heat treatment technology, and cellular structure to improve the high-temperature magnetic performance of a Sm_2Co_{17}-type magnet.[6−12] A new Sm_2Co_{17}-type magnet with the Sm/Co atomic ratio to 1:7 has been developed with a coercivity about 11.6 kOe (1 Oe=79.5775 A/m) at room temperature and 10.8 kOe at 500 °C.[13]

When the Sm_2Co_{17}-type permanent magnet is used over 300 °C, undesirable oxidation will remarkably influence its high-temperature magnetic properties. Pragnell *et al.* systematically investigated the oxidation morphology and oxidation kinetics of $Sm(Co_{0.63}, Fe_{0.27}, Cu_{0.08}, Zr_{0.02})_{8.35}$ and $Sm(Co_{0.74}, Fe_{0.1}, Cu_{0.12}, Zr_{0.04})_{8.5}$ magnets at temperatures ranging from 300 °C to 600 °C in air.[14−16] However, the relation between the oxidation microstructure and maximum energy product $(BH)_{max}$ loss of Sm_2Co_{17}-type magnets has been rarely reported. In this paper, the oxidation microstructure and $(BH)_{max}$ loss of a $Sm(Co_{0.76}, Fe_{0.1}, Cu_{0.1}, Zr_{0.04})_7$ magnet are systematically investigated at 500 °C. An oxygen diffusion model is proposed to simulate the dependence of $(BH)_{max}$ loss on oxidation time.

2. Experiments

The conventional powder metallurgical technique was adopted for the manufacturing of the $Sm(Co_{0.76}, Fe_{0.1}, Cu_{0.1}, Zr_{0.04})_7$ magnet. The ingot with nominal composition was prepared by arc melting with an excess Sm of 10% to compensate for the weight loss. The ingot was crushed into powder of a size ∼ 300 μm for high-energy ball milling. The milling was carried

*Project supported by the National High Technology Research and Development Program of China (Grant No. 2010AA03A401), the National Natural Science Foundation of China (Grant No. 51071010), the Aviation Foundation of China (AFC) (Grant No. 2009ZF51063), and the Fundamental Research Funds for the Central Universities.

†Corresponding author. E-mail: jiangcb@buaa.edu.cn

© 2011 Chinese Physical Society and IOP Publishing Ltd

out under an acetate atmosphere for 1 h with a ball-to-powder weight ratio of 5:1. The as-milled powders were filled in a rubber mold, aligned in a magnetic field up to 5 T and then isostatically compacted under an external pressure of $\sim$ 300 MPa. The degassed powder compaction was sintered and homogenized at 1199 °C for 5 h. The alloy was then isothermally aged at about 800 °C for 24 h, cooled slowly at a rate of 0.7 °C/min to 400 °C and aged at 400 °C for 10 h.

The as-prepared $Sm(Co_{0.76}, Fe_{0.1}, Cu_{0.1}, Zr_{0.04})_7$ magnet was cut into specimens, each with a size of 10 mm×10 mm×2.5 mm for oxidation test. All of the specimens were polished to a 2000-grit finish and cleaned ultrasonically in ethanol before being placed in alumina tubes. The oxidation test was carried out in air at a temperature of 500 °C for up to 500 h. The phase constituents of the oxidized magnet were identified by X-ray diffraction (XRD, D/Max-2200PC) with Cu Kα radiation. The cross-sectional morphologies of the oxidized magnets were examined with scanning electron microscope (FEI Quanta 600) equipped with an energy dispersive X-ray apparatus (EDAX Genesis). Cylindrical specimens of 3 mm×3 mm were prepared for the magnetic measurements. The specimens were magnetized in a 10-T pulsed field before being measured in a vibrating sample magnetometer up to 3 T. No demagnetization corrections were applied to the magnetic measurement results.

3. Results and discussion

3.1. Oxidation microstructure

Figure 1(a) shows the typical cross-sectional backscattered electron image of a $Sm(Co_{0.76}, Fe_{0.1}, Cu_{0.1}, Zr_{0.04})_7$ magnet oxidized at 500 °C for 200 h. It can be seen that the oxidized $Sm(Co_{0.76}, Fe_{0.1}, Cu_{0.1}, Zr_{0.04})_7$ magnet consists of a continuous external oxide scale, an internal reaction layer (IRL), and a diffusion zone (DZ). The phase constituents for the three regions above are identified by the XRD patterns, as shown in Fig. 2. The crystal structure of unaffected base alloy was also given for comparison. In the external oxide scale, the phase constitution is mainly composed of $CoFe_2O_4$, Co_3O_4, and CuO, as shown in Fig. 2(a). The IRL consists of Sm_2O_3 and a FeCo matrix suggested by the XRD pattern in Fig. 2(b). Moreover, Co/Cu-rich long precipitates within the IRL can be observed at the grain boundaries, as shown in Fig. 1(b), while the DZ has the phase structure of Sm_2Co_{17} and $SmCo_5$ similar to the unaffected base alloy [Figs. 2(c) and 2(d)].

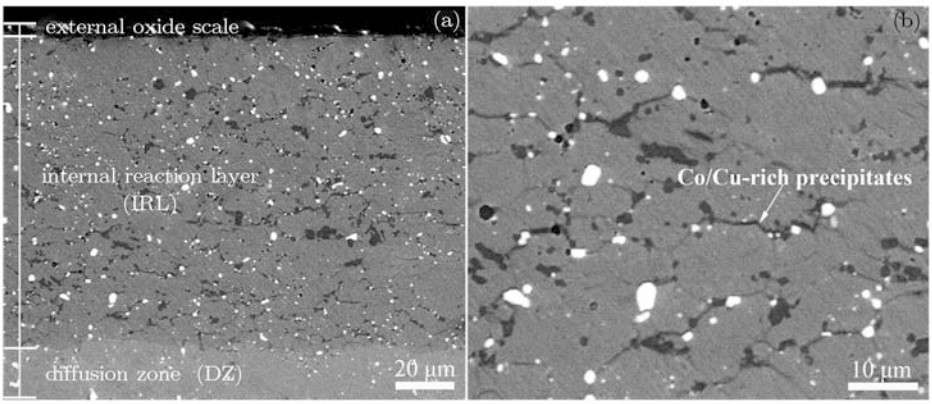


Fig. 1. The typical cross-sectional backscattered electron images of a $Sm(Co_{0.76}, Fe_{0.1}, Cu_{0.1}, Zr_{0.04})_7$ magnet oxidized at 500 °C for 200 h: (a) overall microstructure, and (b) a magnified view of the IRL.

After oxidation at 500 °C for 200 h, the thickness of external oxide scale is about 5 μm [Fig. 1(a)], which increases slightly with oxidation time. On the other hand, the thickness of IRL is about 106 μm [Fig. 1(a)], which will grow drastically with the increase of oxidation time. Since the $Sm(Co_{0.76}, Fe_{0.1}, Cu_{0.1}, Zr_{0.04})_7$ magnet exhibits easy-magnetization and hard-magnetization directions parallel and perpendicular to the c axis, respectively, the thickness kinetics of IRL in both directions were measured, as shown in Fig. 3. It can be seen that the thicknesses of IRL in both directions exhibits a parabolic increase with oxidation time. Moreover, the difference of the thickness kinetics of IRL between the above two directions is slight. Therefore, the thickness kinetics equation of IRL for both directions can be fitted as follows:

$$L_1(t) = (kt)^{1/2}, \tag{1}$$

where $L_1(t)$ denotes the thickness of IRL, k is the oxidation rate constant, and t is the oxidation time. The value of the average oxidation rate constant k for the $Sm(Co_{0.76}, Fe_{0.1}, Cu_{0.1}, Zr_{0.04})_7$ magnet is about 1.91×10^{-10} cm^2/s.

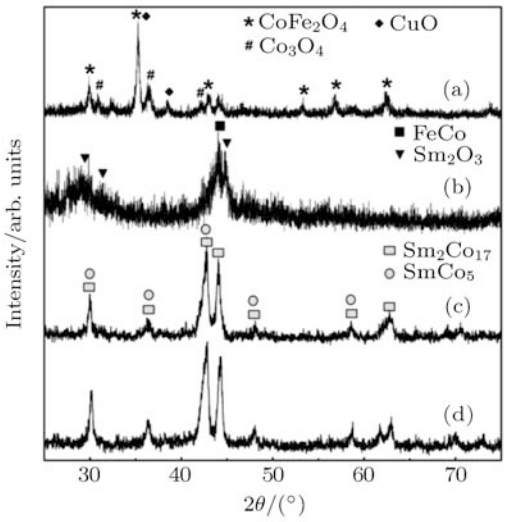


Fig. 2. XRD patterns of the oxidized a $Sm(Co_{0.76}, Fe_{0.1}, Cu_{0.1}, Zr_{0.04})_7$ magnet at 500 °C for different regions: (a) external oxide scale, (b) IRL, (c) DZ, and (d) unaffected base alloy.

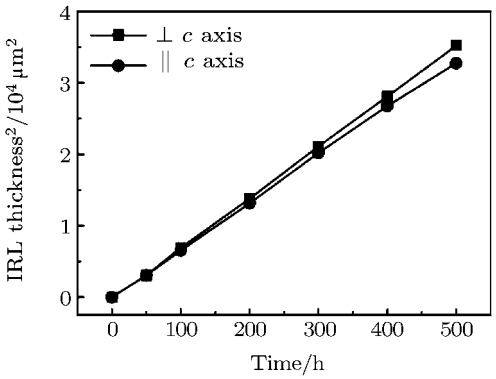


Fig. 3. Dependence of the IRL thickness squared on oxidation time at 500 °C.

3.2. Maximum energy product $(BH)_{max}$ loss

As the microstructure of the $Sm(Co_{0.76}, Fe_{0.1}, Cu_{0.1}, Zr_{0.04})_7$ magnet changed during the oxidation process at 500 °C, it will have a large effect on the magnetic performance. A cylindrical specimen of 3 mm×3 mm was prepared for the magnetic measurements. Figure 4(a) shows the variation of room-temperature demagnetization curves and B–H curves with oxidation time for the oxidized $Sm(Co_{0.76}, Fe_{0.1}, Cu_{0.1}, Zr_{0.04})_7$ magnet. It can be seen that with the increase of oxidation time, the room-temperature remanence M_r and intrinsic coercivity ${}_iH_c$ remarkably decrease. Moreover, the room-temperature B–H curves exhibited a decrease with oxidation time, where they dropped drastically from 0 h to 200 h and slowly from 200 h to 500 h, as shown in Fig. 4(a). Similar decreases in the high-temperature demagnetization curves and B–H curves at 500 °C were observed in Fig. 4(b). Besides, the high-temperature B–H curves are kept straight during the whole oxidation process [Fig. 4(b)], indicating that the maximum operating temperature of the $Sm(Co_{0.76}, Fe_{0.1}, Cu_{0.1}, Zr_{0.04})_7$ magnet is up to 500 °C.

Figure 4(c) shows the dependence of the $(BH)_{max}$ loss squared (at room temperature and 500 °C) on oxidation time. It can be seen that both the room-temperature and high-temperature $(BH)_{max}$ losses as functions of oxidation time follow a parabolic law. Moreover, the difference in $(BH)_{max}$ losses between the room-temperature and high-temperature measurements is quite small and can be ignored. Therefore, the $(BH)_{max}$ loss as a function of oxidation time at the two temperatures can be fitted as follows:

$$(BH)_{max}\,\text{loss}\,(t) = -6.0\times10^{-4}t^{1/2}. \qquad (2)$$

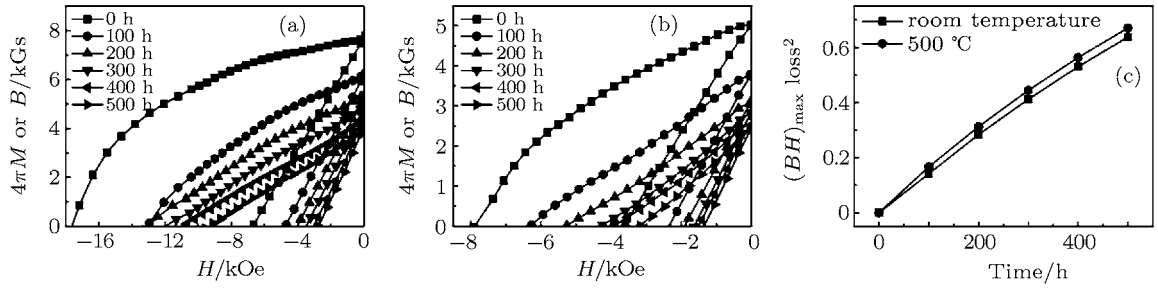


Fig. 4. Variations of demagnetization curves and B–H curves with the oxidation time at (a) room temperature and (b) 500 °C for the oxidized $Sm(Co_{0.76}, Fe_{0.1}, Cu_{0.1}, Zr_{0.04})_7$ magnet. Panel (c) shows the dependence of the $(BH)_{max}$ loss squared (at room temperature and 500 °C) on oxidation time (1 Gs=10^4 T).

3.3. Oxygen diffusion model

Figure 5 shows the typical oxygen diffusion model in the oxidized $Sm(Co_{0.76}, Fe_{0.1}, Cu_{0.1}, Zr_{0.04})_7$ magnet at 500 °C. According to the oxidation microstructure in Fig. 1, there are three different regions formed in the oxidized magnet: the continuous external oxide scale, IRL, and DZ. Since the thickness of the external oxide scale is quite thin and increases slightly with oxidation time compared with that of IRL, it is ignored in the oxygen diffusion model. Therefore, the diffusion of oxygen in the oxidized $Sm(Co_{0.76}, Fe_{0.1}, Cu_{0.1}, Zr_{0.04})_7$ magnet can be simplified to a typical diffusion model in binary systems with one fixed and one moving boundary.[17] The boundary between the external surface and IRL is fixed. Contrarily, the interface boundary between the IRL and DZ is moving due to the increased thickness of IRL with oxidation time. According to the Matano–Boltzmann method with non-stationary boundaries,[17] the diffusion coefficient D of oxygen in the above model can be regarded as a constant and the length of DZ can be written as follows:

$$L_2(t) = 2(Dt)^{1/2}, \tag{3}$$

where $L_2(t)$ denotes the length of DZ.

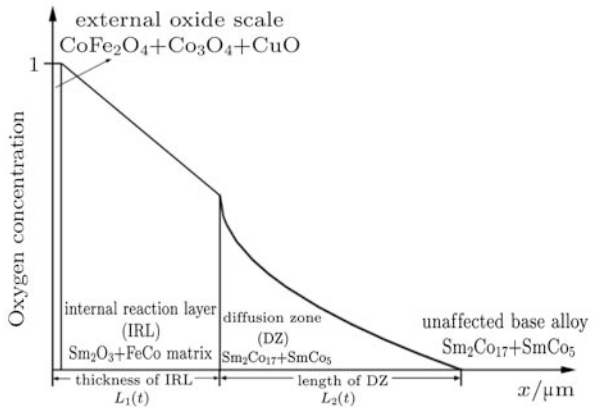


Fig. 5. The typical oxygen diffusion model in the oxidized $Sm(Co_{0.76}, Fe_{0.1}, Cu_{0.1}, Zr_{0.04})_7$ magnet at 500 °C.

Since the $(BH)_{max}$ loss is proportional to the volume consumed by the whole oxidation region including the IRL and DZ, the relationship between the $(BH)_{max}$ loss and oxidation time is proposed as follows:[18]

$$(BH)_{max}\,\text{loss}(t) = -\left(\frac{S}{V}\right)[L_1(t) + L_2(t)], \tag{4}$$

where (S/V) is the ratio of surface area to volume. By substituting Eqs. (1) and (3) into Eq. (4), the $(BH)_{max}$ loss as a function of oxidation time can be written as follows:

$$(BH)_{max}\,\text{loss}(t) = -\left(\frac{S}{V}\right)\left[k^{1/2} + 2D^{1/2}\right]t^{1/2}. \tag{5}$$

Since the oxidation rate constant k and oxygen diffusion coefficient D are independent of the local crystallographic c-axis orientation, the variation of $(BH)_{max}$ loss with oxidation time for the $Sm(Co_{0.76}, Fe_{0.1}, Cu_{0.1}, Zr_{0.04})_7$ magnet with different shapes and sizes can be written as follows:

$$\left(\frac{V}{S}\right)(BH)_{max}\,\text{loss}(t) = -\left[k^{1/2} + 2D^{1/2}\right]t^{1/2}(\text{cm}). \tag{6}$$

The value of (V/S) is equal to 0.05 cm in our experiment due to the cylindrical specimens of 3 mm×3mm for the magnetic measurement. By comparing Eq. (6) with Eq. (2) and substituting the oxidation rate constant $k = 1.91 \times 10^{-10}$ cm^2/s, the oxygen diffusion coefficient D is obtained, which is about 6.54×10^{-11} cm^2/s.

Based on Eq. (6) with the values of oxidation rate constant k and oxygen diffusion coefficient D, the contributions of both IRL and DZ to the $(BH)_{max}$ loss at different oxidation time are calculated and listed in Table 1, respectively. It can be seen that the DZ leads to more $(BH)_{max}$ loss than the IRL during the whole oxidation process. Therefore, more attention will be paid to inhibit the oxygen diffusion in the Sm_2Co_{17} magnet to improve its oxidation resistance during the oxidation process and these studies are underway.

Table 1. Comparison of the $(BH)_{max}$ loss arising from the IRL and DZ for the oxidized $Sm(Co_{0.76}, Fe_{0.1}, Cu_{0.1}, Zr_{0.04})_7$ magnet with different shapes and sizes at 500 °C.

Oxidation time/h	$(BH)_{max}$ loss by IRL/(% cm)	$(BH)_{max}$ loss by DZ/(% cm)
100	–0.83	–0.97
200	–1.17	–1.37
300	–1.44	–1.68
400	–1.66	–1.94
500	–1.86	–2.17

4. Conclusion

In summary, the relation between the oxidation microstructure and maximum energy product $(BH)_{max}$ loss of the oxidized $Sm(Co_{0.76}, Fe_{0.1}, Cu_{0.1}, Zr_{0.04})_7$ magnet at 500 °C were studied. A general equation $(V/S)(BH)_{max}\,\text{loss}(t) = -\left[k^{1/2} + 2D^{1/2}\right]t^{1/2}(\text{cm})$ was proposed to predict the variation of $(BH)_{max}$ loss with the oxidation time for the Sm_2Co_{17} magnets with different shapes and sizes. For the $Sm(Co_{0.76}, Fe_{0.1}, Cu_{0.1}, Zr_{0.04})_7$ magnet, the values of both oxidation rate constant k and oxygen diffusion coefficient D are about 1.91×10^{-10} cm^2/s and 6.54×10^{-11} cm^2/s, respectively.

References

[1] Kim A S 1998 *J. Appl. Phys.* **83** 6715

[2] Liu J F, Zhang Y, Dimitrov D and Hadjipanayis G C 1999 *J. Appl. Phys.* **85** 2800

[3] Chen R J, Zhang H W, Rong C B, Sun J R and Shen B G 2006 *J. Appl. Phys.* **100** 043901

[4] Chen C H, Walmer M S, Walmer M H, Liu S, Kuhl E and Simon G 1998 *J. Appl. Phys.* **83** 6706

[5] Feng H B, Chen H S, Guo Z H, Pan W, Zhu M G and Li W 2011 *J. Appl. Phys.* **109** 07A763

[6] Gutfleisch O, Müller K H, Khlopkov K, Wolf M, Yan A, Schäfer R, Gemming T and Schultz L 2006 *Acta Mater.* **54** 997

[7] Ma B M, Liang Y L and Bounds C O 1997 *J. Appl. Phys.* **81** 5612

[8] Guo Z H, Pan W and Li W 2006 *J. Magn. Magn. Mater.* **303** e396

[9] Liu T, Guo Z H, Li X M and Li W 2009 *Acta Phys. Sin.* **58** 2030 (in Chinese)

[10] Tang W, Zhang Y and Hadjipanayis G C 2000 *J. Appl. Phys.* **87** 399

[11] Li X M, Fang Y K, Guo Z H, Liu T, Guo Y Q, Li W and Han B S 2008 *Chin. Phys.* B **17** 2281

[12] Liu T and Li W 2009 *Acta Phys. Sin.* **58** 5773 (in Chinese)

[13] Liu J F, Ding Y, Zhang Y, Dimitar D, Zhang F and Hadjipanayis G C 1999 *J. Appl. Phys.* **85** 5660

[14] Pragnell W M, Williams A J and Evans H E 2008 *J. Appl. Phys.* **103** 07E127

[15] Pragnell W M, Evans H E and Williams A J 2009 *J. Alloys Compd.* **473** 389

[16] Pragnell W M, Williams A J and Evans H E 2009 *J. Alloys Compd.* **487** 69

[17] Kubíček P and Mrázek L 1998 *Czech. J. Phys.* **48** 1049

[18] Liu L L and Jiang C B 2011 *Appl. Phys. Lett.* **98** 252504